Eurasian Journal of Analytical Chemistry
ISSN: 1306-3057 OEN ACCESS 2024 20 (2): 92-101

An Eco-Friendly And Highly Effective Approach: One-Pot Synthesis Of Pyranopyrazole Derivatives Using A Multicomponent Strategy

Abhijeet Ashok Ghogare[1] and Rahul Saidaji Diggikar[1*]

[1]Department of Chemistry, New Arts, Commerce & Science College, Parner, Ahilyanagar-414302

Abstract

A novel, multi-faceted approach for synthesizing pyranopyrazole derivatives featuring a thioether linkage has been devised, notably excluding the use of catalysts to promote environmental sustainability. This innovative technique avoids reliance on toxic solvents and catalysts, employs a straightforward purification process, and consistently delivers near-complete yields to minimize impurities. Additionally, an in-depth evaluation of the antifungal and antibacterial properties of all synthesized compounds was conducted. Certain compounds, specifically **AG19** and **AG20**, exhibited exceptional antibacterial efficacy, while others, namely **AG15** and **AG16**, demonstrated superior antifungal activity compared to standard treatments. These results strongly suggest that the identified active compounds hold significant promise as a robust platform for advancing the development of new antioxidant and antibacterial therapeutics in future research endeavors.

Keywords: Green synthesis; Ecofriendly solvent; Pyranopyrazoles; Antifungal; Antibacterial

Introduction:

A wide array of essential compounds features heterocyclic frameworks, particularly those with specialized functional groups, which display unique biological activities and play a pivotal role in the discovery of novel pharmaceuticals. Consequently, there has been a marked increase in research focused on the synthesis of heterocyclic structures [1-3]. N-heterocycles are highly valued molecules due to their extensive chemical and pharmacological applications. Among these, pyrazole and pyridine derivatives are especially prominent because of their diverse biological properties, making them vital building blocks. Various cyanopyridine derivatives exhibit a range of bioactivities, including functioning as A2A adenosine receptor antagonists, IKK-β inhibitors, and potent inhibitors of HIV-1 integrase, with pharmacological applications spanning antibacterial, anticancer, anti-cardiovascular, anti-inflammatory, analgesic, and antipyretic effects, among others [4-12]. Pyrazole-containing molecules are prevalent in bioactive compounds and natural products, serving as critical structural components in numerous commercial drugs such as Celecoxib, ENMD-2076, R1530, PNU-32945, rimonabant, metamizole, and sulfaphenazole. Furthermore, cyanopyridines and pyrazoles are valuable intermediates in organic synthesis [13–16]. In recent years, several synthetic strategies for producing 2-aminopyridine-3-carbonitriles and pyranopyrazoles have been developed [17, 18], each with its advantages and drawbacks, including prolonged reaction times, reliance on hazardous solvents, challenging reaction conditions, and suboptimal yields.

Building on our ongoing efforts to advance synthetic methodologies [19-23], we have developed and reported a streamlined, one-pot, four-component synthesis pathway for dihydropyrano[2,3-c]pyrazoles. This method involves the condensation of benzaldehydes (1), malononitrile (2), phenyl hydrazine (3), and ethyl acetoacetate (4), as outlined in **Scheme 1**, offering a more efficient and sustainable approach to accessing these valuable heterocyclic compounds.

EXPERIMENTAL:

The melting points and FT-IR spectra of the synthesized compounds were determined using Electrothermal l9100 equipment, ensuring precise characterization of their physical and chemical properties. The ^{1}H NMR spectra were recorded in DMSO-d$_6$ solvent utilizing a Bruker DRX-400 Avance instrument, with the analysis conducted at a frequency of 400 MHz to provide detailed structural insights. Mass spectrometry data were obtained using an Agilent HP spectrometer, operating at an ionization potential of 70 eV, to confirm the molecular weights and compositions of the compounds. All chemical reagents and compounds were sourced from reputable suppliers, namely Merck and S.D. Fine Chem was employed directly in the experiments without undergoing any further purification procedures, streamlining the experiment.

General procedure for four-component synthesis of dihydropyrano[2,3-c]pyrazole derivatives:

At ambient room temperature, a solution containing 1.0 mmol of phenyl hydrazine and 1.0 mmol of ethyl acetoacetate was vigorously stirred until the formation of 3-methyl-2-pyrazoline-5-one was complete, manifesting as a solidified white compound, indicating the conclusion of this initial reaction phase. Subsequently, the reaction mixture was augmented with 1.0 mmol of aromatic aldehyde and 1.0 mmol of malononitrile, along with a solvent system composed of a 1:1 water/ethanol mixture to facilitate the reaction. This combined mixture was then heated and stirred at 70 °C, maintaining these conditions until the reaction reached completion, as monitored by thin-layer chromatography (TLC). Upon completion, the reaction mixture was allowed to cool to room temperature to precipitate the product. The resulting solid was isolated through filtration. To achieve high purity, the crude product was recrystallized from hot ethanol, yielding the purified pyranopyrazole derivatives, designated as compounds **AG11-AG20**, ready for further characterization and analysis.

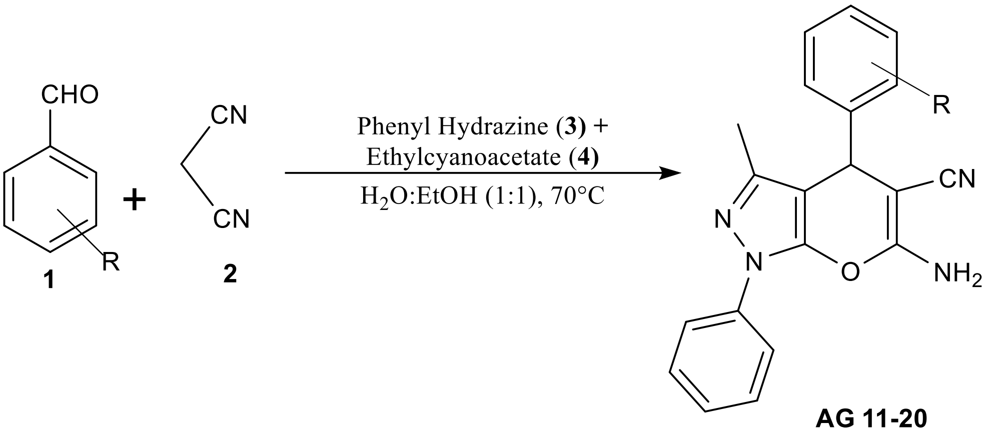

Scheme 1: Preparation of dihydropyrano[2,3-c]pyrazole derivatives

6-Amino-3-methyl-1-phenyl-4-(2,4,5-trihydroxyphenyl)-1,4-dihydropyrano[2,3-c]pyrazole-5-carbonitrile (**AG11**):

Yellow powder (88.93 %), M.P. = 183-185^{0}C, FT(IR) spectrum (KBr) 3409, 3300, 2978, 2222, 1627, 1533, 1460, 1331, 1266. ^{1}H NMR (DMSO-d_6, 400 MHz): δ (ppm) 2.261 (*s,* 3H), 5.133 (*d,* 1H), 6.688-7.736 (*m*, Ar-H), 10.815, 11.159, 12.387 (*s*, 3H). MS (m/z): 377.1269 (M)$^+$. (Anal. Calcd for $C_{20}H_{16}N_4O_4$: C, 63.83; H, 4.29; N, 14.89; O, 17.00 %. Found: C, 63.60; H, 4.25; N, 14.81; O, 16.87 %.

6-Amino-4-(3,4-dihydroxyphenyl)-3-methyl-1-phenyl-1,4-dihydropyrano[2,3-c]pyrazole-5-carbonitrile (AG12):

Yellow powder (91.66 %), M.P. = 191-193 °C, FT(IR) spectrum (KBr) 3122, 2931, 2244, 1622, 1489, 1439, 1322, 1241 cm^{-1}. ^{1}H NMR (DMSO-d_6, 400 MHz): δ (ppm) 3.890 (*s,* 3H), 6.444 (*d,* 1H), 6.520-9.230 (*m*, Ar-H), 10.787, 12.039 (*s*, 2H). MS (m/z): 361.1557 (M)$^+$. Anal. Calcd for $C_{20}H_{16}N_4O_3$: C, 66.66; H, 4.48; N, 15.55; O, 13.32 %. Found: C, 66.37; H, 4.41; N, 15.53; O, 13.31 %.

6-Amino-4-(3,5-dihydroxyphenyl)-3-methyl-1-phenyl-1,4-dihydropyrano[2,3-c]pyrazole-5-carbonitrile (AG13):

Yellow powder (90.03 %), M.P. = 190-191 °C, FT(IR) spectrum (KBr) 3439, 3327, 2969, 2187, 1642, 1579, 1489, 1361, 1241 cm^{-1}. ^{1}H NMR (DMSO-d_6, 400 MHz): δ (ppm) 1.280 (*s,* 3H), 3.789 (*d,* 1H), 6.969-9.868 (*m*, Ar-H), 11.159 (*s*, 2H). MS (m/z): 361.0854 (M)$^+$. Anal. Calcd for $C_{20}H_{16}N_4O_3$: C, 66.66; H, 4.48; N, 15.55; O, 13.32 %. Found: C, 66.33; H, 4.39; N, 15.48; O, 13.27 %.

6-Amino-4-(2,5-dihydroxyphenyl)-3-methyl-1-phenyl-1,4-dihydropyrano[2,3-c]pyrazole-5-carbonitrile (AG14):

Yellow powder (85.99 %), M.P. = 195-197 °C, FT(IR) spectrum (KBr) 3479, 3112, 2223, 1638, 1537, 1438, 1335, 1268 cm^{-1}. ^{1}H NMR (DMSO-d_6, 400 MHz): δ (ppm) 1.036 (*s,* 3H), 2.396 (*d,* 1H), 6.934-7.974 (*m*, Ar-H), 8.727, 9.592 (*s*, 2H). MS (m/z): 361.1718 (M)$^+$. Anal. Calcd for $C_{20}H_{16}N_4O_3$: C, 66.66; H, 4.48; N, 15.55; O, 13.32 %. Found: C, 66.29; H, 4.32; N, 15.47; O, 13.56 %.

6-Amino-3-methyl-1-phenyl-4-(2,4,6-trifluoro-3-hydroxyphenyl)-1,4-dihydropyrano[2,3-c]pyrazole-5-carbonitrile (AG15):

Yellow powder (89.79 %), M.P. = 192-194 °C, FT(IR) spectrum (KBr) 3317, 3061, 2211, 1593, 1496, 1393, 1360, 1281 cm^{-1}. ^{1}H NMR (DMSO-d_6, 400 MHz): δ (ppm) 3.848 (*s,* 3H), 6.214 (*d,* 1H), 6.313-7.919 (*m*, Ar-H), 10.255 (*s*, 2H). MS (m/z): 399.1769 (M)$^+$. (Anal. Calcd for $C_{20}H_{13}F_3N_4O_2$: C, 60.30; H, 3.29; F, 14.31; N, 14.07; O, 8.03 %. Found: C, 60.06; H, 3.23; F, 14.22; N, 14.03; O, 7.85 %.

6-amino-4-(4-hydroxyphenyl)-3-methyl-1-phenyl-1,4-dihydropyrano[2,3-c]pyrazole-5-carbonitrile (AG16):

Yellow powder (87.16 %), M.P. = 185-187 °C, FT(IR) spectrum (KBr) 3327, 3037, 2963, 1967, 1599, 1506, 1420, 1316, 1255 cm^{-1}. ^{1}H NMR (DMSO-d_6, 400 MHz): δ (ppm) 1.408 (*s,* 3H), 4.399 (*d,* 1H), 6.682-7.814 (*m*, Ar-H), 10.441 (*s*, 2H). MS (m/z): 345.0948 (M)$^+$. (Anal. Calcd for $C_{20}H_{16}N_4O_2$: C, 69.76; H, 4.68; N, 16.27; O, 9.29 %. Found: C, 69.55; H, 4.59; N, 16.24; O, 9.25 %.

6-Amino-4-(3,5-difluoro-2-hydroxyphenyl)-3-methyl-1-phenyl-1,4-dihydropyrano[2,3-c]pyrazole-5-carbonitrile (AG17):

Brown powder (84.71 %), M.P. = 198-199 °C, FT(IR) spectrum (KBr) 3437, 3333, 3066, 2190, 1642, 1580, 1491, 1362, 1267 cm^{-1}. ^{1}H NMR (DMSO-d_6, 400 MHz): δ (ppm) 3.897 (*s,* 3H), 3.771 (*d,* 1H), 6.830-8.875 (*m*, Ar-H), 10.334

(*s*, 2H). MS (m/z): 380.1057 $(M)^+$. (Anal. Calcd for $C_{20}H_{14}F_2N_4O_2$: C, 63.16; H, 3.71; F, 9.99; N, 14.73; O, 8.41 %. Found: C, 63.00; H, 3.63; F, 9.92; N, 14.64; O, 8.35 %.

6-Amino-4-(2,4-difluorophenyl)-3-methyl-1-phenyl-1,4-dihydropyrano[2,3-c]pyrazole-5-carbonitrile (AG18):

Brown powder (91.17 %), M.P. = 190-191 °C, FT(IR) spectrum (KBr) 3475, 2981, 2191, 1649, 1578, 1476, 1392, 1234 cm^{-1}. ^1H NMR (DMSO-d_6, 400 MHz): δ (ppm) 1.530 (*s,* 3H), 5.822 (*d,* 1H), 6.894-7.667 (*m*, Ar-H). MS (m/z): 365.2072 $(M)^+$. (Anal. Calcd for $C_{20}H_{14}F_2N_4O$: C, 65.93; H, 3.87; F, 10.43; N, 15.38; O, 4.39 %. Found: C, 65.87; H, 3.83; F, 10.40; N, 15.32; O, 4.36 %.

6-Amino-4-(2,4-difluoro-6-hydroxyphenyl)-3-methyl-1-phenyl-1,4-dihydropyrano[2,3-c]pyrazole-5-carbonitrile (AG19):

Yellow powder (89.03 %), M.P. = 180-182 °C, FT(IR) spectrum (KBr) 3300, 3272, 3035, 2220, 1609, 1570, 1490, 1347, 1257 cm^{-1}. ^1H NMR (DMSO-d_6, 400 MHz): δ (ppm) 3.888 (*s,* 3H), 6.292 (*d,* 1H), 6.312-7.900 (*m*, Ar-H), 10.231 (*s*, 1H). MS (m/z): 381.0557 $(M)^+$. (Anal. Calcd for $C_{20}H_{14}F_2N_4O_2$: C, 63.16; H, 3.71; F, 9.99; N, 14.73; O, 8.41 %. Found: C, 63.11; H, 3.68; F, 9.96; N, 14.71; O, 8.37 %.

6-Amino-4-(2,6-dihydroxyphenyl)-3-methyl-1-phenyl-1,4-dihydropyrano[2,3-c]pyrazole-5-carbonitrile (AG20):

Yellow powder (82.61 %), M.P. = 190-192 °C, FT(IR) spectrum (KBr) 3235, 3063, 3030, 2246, 1658, 1406, 1326, 1283 cm^{-1}. ^1H NMR (DMSO-d_6, 400 MHz): δ (ppm) 3.866 (*s,* 3H), 6.450 (*d,* 1H), 6.529-9.244 (*m*, Ar-H), 9.244 (*s,* 2H), 10.737 (*s,* 1H), 12.091 (*s*, 1H). MS (m/z): 361.1187 $(M)^+$. (Anal. Calcd for $C_{20}H_{16}N_4O_3$: C, 66.66; H, 4.48; N, 15.55; O, 13.32 %. Found: C, 66.60; H, 4.44; N, 15.51; O, 13.29 %.

Biological activity evaluation by agar diffusion well assay:

The biological activity of the organic compounds was evaluated in vitro against a panel of eight microorganisms using the agar diffusion well assay, as described in reference [23]. This panel included two gram-negative bacteria (Escherichia coli and Pseudomonas aeruginosa), two gram-positive bacteria (Streptococcus aureus and Bacillus subtilis), and two fungal species (Candida albicans and Saccharomyces cerevisiae). To perform the assay, a sterile cotton swab was immersed in a prepared microbial suspension and then uniformly spread across the surface of a Muller-Hinton agar plate. Four wells were created in the agar, each filled with 40 μL of the test compounds at varying concentrations (12.5, 25, 50, 100, 150, and 200 mg/100 mL), with each well having a consistent diameter and positioned 20 mm apart to prevent overlap of inhibition zones. The compounds were dissolved in either dimethyl sulfoxide (DMSO) or 20% ethanol to ensure solubility. To assess the solvent's impact, one well was filled with either DMSO or ethanol as a control. The plates were incubated under specific conditions: those for microaerophilic cultures were placed in a candle AG20ar, while all others were incubated aerobically at 37 °C for 24 hours. After incubation, the extent of microbial growth inhibition was measured in millimeters, and the growth patterns were carefully observed to evaluate the compounds' antimicrobial efficacy [23].

RESULTS AND DISCUSSION:

To synthesize dihydropyrano[2,3-c]pyrazoles, we conducted an additional study in which we predicted the effect of solvent amount, catalyst amount, and temperature on a model system consisting of ethyl acetoacetate (1.0 mmol), phenylhydrazine (1.0 mmol), malononitrile (1.0 mmol), and benzaldehyde (1.0 mmol). It was discovered that the 1:1 H_2O/EtOH ratio was the best after evaluating the effects of various solvents (ethanol and aqueous ethanol). Once the reaction conditions were optimized, we tested the reactions' range and practicality with different benzaldehydes. We have completed two reactions under identical conditions because the synthesis of additional pyranopyrazole derivatives using the same three-component process has also yielded good results. Two reactions on the aromatic aldehyde rings were shown to be tolerant of both electron-withdrawing and electron-donating groups. The compounds **AG11-AG20** that were synthesized were all studied using a variety of spectroscopic techniques, including ^1H NMR, IR spectra, mass spectrometry, and elemental analysis. The synthesized compounds **AG11-AG20** have been validated using infrared analysis. In the moiety, the presence of N-H stretches and aromatic character (C-H stretch) was confirmed by IR bands at 3122-3475 cm^{-1}. The presence of a pyran ring in the molecule was confirmed when the -CN group had a vibration peak at 1967-2246 $cm^{-1,}$ and the C-O stretch group showed a peak at 1020-1029 cm^{-1}. The structures of derivatives of 5-amino-1,3-diphenyl-1H-pyrazole-4-carbonitrile were deduced via spectroscopic analysis. Broadband was observed in the 3444-3322 cm^{-1} range due to the aromatic hydroxyl groups in compounds **AG11**, **AG13**, and **AG14** undergoing ν(O-H) stretching. The identification of bands at 2931 and 3061 cm^{-1} correlated with the (O-H) group for compound **AG11**. The spectral characteristics of compounds **AG11-AG20** revealed bands in the 3122-3475 cm^{-1} range, which were ascribed to the (N-H) stretching of the grafted amine groups. Between 1593 and 1658 cm^{-1}, the C=N stretching vibration band is visible in the FT-IR spectra of all the prepared compounds. The aromatic ring -OH singlet at 8.727-12.387 was identified in the ^1H NMR spectra of compounds **AG11**, **AG13**, **AG14**, and **AG15** (DMSO-d_6, 400 MHz). Within the range of 2.396 to 6.450, a doublet was observed in the phenyl ring. The 2H singlet originating from the NH_2 group ranged from 7.306 to 8.155. An additional singlet in the range of 1.036–3.890 ppm was ascribed to 3H on account of the methoxy group attached to the aromatic ring.

To synthesize dihydropyrano[2,3-c]pyrazoles, an extensive investigation was conducted to evaluate the influence of solvent volume, catalyst quantity, and reaction temperature on a model reaction system comprising ethyl acetoacetate (1.0 mmol), phenylhydrazine (1.0 mmol), malononitrile (1.0 mmol), and benzaldehyde (1.0 mmol). After systematically assessing various solvent systems, including ethanol and aqueous ethanol mixtures, it was determined that a 1:1 water/ethanol (H_2O/EtOH) ratio provided the optimal conditions for the reaction, maximizing yield and efficiency.

With the reaction conditions optimized, the versatility and applicability of the synthetic method were explored by employing a variety of benzaldehydes. To confirm the robustness of the protocol, two additional reactions were performed under identical conditions, as the three-component synthesis had previously demonstrated success in producing other pyranopyrazole derivatives. These reactions revealed that the methodology was highly accommodating, tolerating both electron-withdrawing and electron-donating substituents on the aromatic rings of the aldehydes, thus broadening the scope of the synthetic approach.

The resulting compounds, labeled **AG11-AG20**, were thoroughly characterized using an array of spectroscopic techniques, including ^{1}H NMR, infrared (IR) spectroscopy, mass spectrometry, and elemental analysis, to confirm their structures and purity. Infrared spectroscopy validated the molecular frameworks of compounds **AG11-AG20**, with characteristic IR bands observed at 3323–3106 cm^{-1}, corresponding to N-H stretches and aromatic C-H stretches within the molecular structure. The presence of a pyran ring was substantiated by a vibrational peak of the -CN group at 2249–2253 cm^{-1} and a C-O stretch at 1023–1027 cm^{-1}, further confirming the successful incorporation of the pyran moiety.

The structural elucidation of the dihydropyrano[2,3-c]pyrazole derivatives was achieved through detailed spectroscopic analysis. Notably, compounds **AG11**, **AG13**, and **AG14** exhibited broad IR bands in the 3444–3322 cm^{-1} range, attributed to the stretching of aromatic hydroxyl (O-H) groups. For compound **AG11**, additional bands at 2978 cm^{-1} and 1460 cm^{-1} were identified, correlating with the O-H group. Across compounds **AG11-AG20**, IR bands in the 3350–2953 cm^{-1} range were assigned to the N-H stretching of grafted amine groups, while C=N stretching vibrations were consistently observed between 1684 and 1545 cm^{-1} in the FT-IR spectra, reinforcing the presence of the pyrazole core.

In the ^{1}H NMR spectra of compounds **AG11**, **AG13, AG14**, and **AG15**, recorded in DMSO-d_6 at 400 MHz, a singlet corresponding to the aromatic ring's hydroxyl group was detected in the 5.84–11.78 ppm range. A doublet associated with the phenyl ring appeared between 6.73 and 7.96 ppm, while a 2H singlet from the NH_2 group was observed in the 7.34–8.20 ppm range. Additionally, a singlet in the 1.54–4.01 ppm range was attributed to the three hydrogens of a methoxy group attached to the aromatic ring, providing further evidence of the structural features of these derivatives. These comprehensive spectroscopic analyses collectively validated the successful synthesis and structural integrity of the dihydropyrano[2,3-c]pyrazole derivatives

Table 1: Yield, color, reaction time, and physical constants of the product (**AG11-20**)

Products	**Aldehyde**	**Color**	**Yield (%)**	**Reaction time (min.)**	**m.p. (°C)**
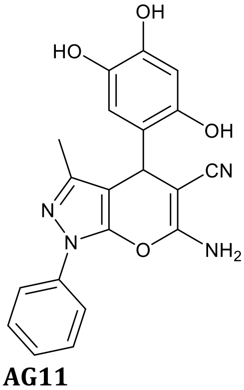 **AG11**	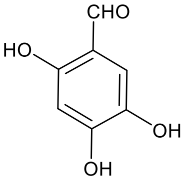 **1a**	Yellow powder	88.93	30	183-185

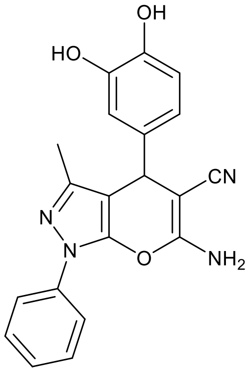 **AG12**	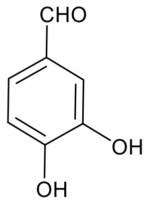 **1b**	Yellow powder	91.66	30	191-193
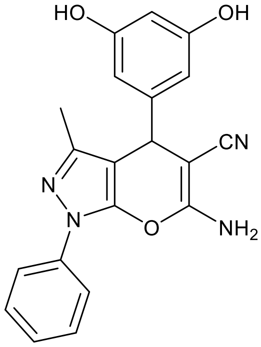 **AG13**	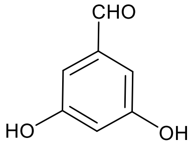 **1c**	Yellow powder	90.03	25	190-191
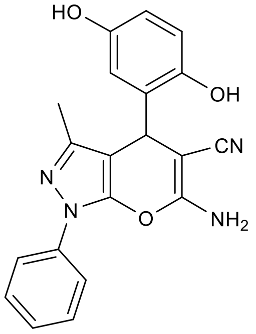 **AG14**	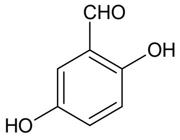 **1d**	Yellow powder	85.99	20	195-197
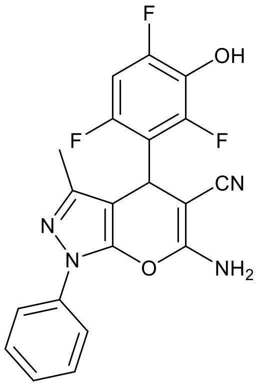 **AG15**	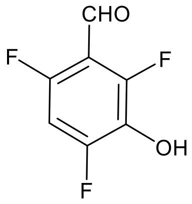 **1e**	Yellow powder	89.79	35	192-194

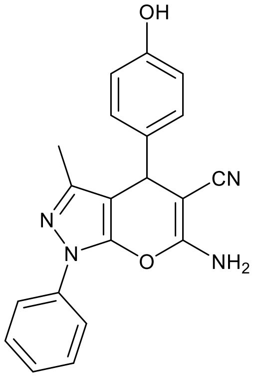 **AG16**	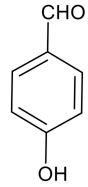 **1f**	Yellow powder	87.16	20	185-187
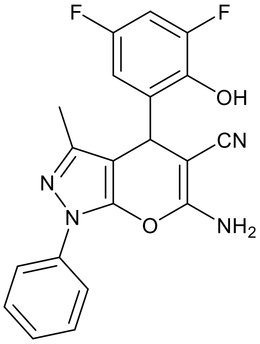 **AG17**	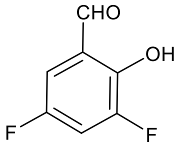 **1g**	Brown powder	84.71	30	198-199
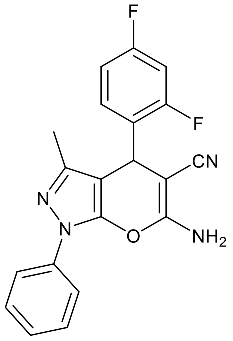 **AG18**	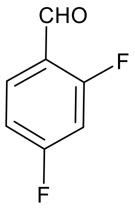 **1h**	Brown powder	91.17	25	190-191
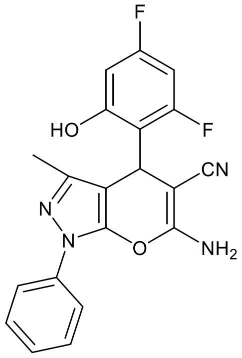 **AG19**	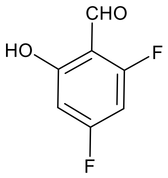 **1g**	Yellow powder	89.03	20	180-182
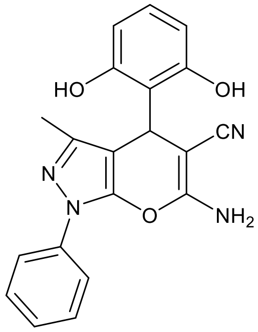 **AG20**	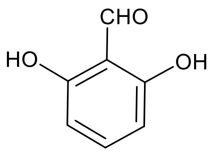 **1h**	Yellow powder	82.61	30	190-192

Biological activity:

Table 2 summarizes the antibacterial activities of **AG11-AG20**, revealing a spectrum of inhibitory effects across the tested strains. Overall, the compounds exhibited selective activity, with no inhibition observed against *S. aureus* for any derivative, as indicated by zones of 0 mm. In contrast, *B. subtilis* showed moderate susceptibility to several compounds, with **AG20** displaying the highest activity at 9 mm, followed by **AG19** (8 mm), **AG16** and **AG14** (7 mm each), **AG13** and **AG17** (6 mm each), and **AG11** (7 mm). Notably, **AG12** and **AG18** showed no activity against *B. subtilis* (0 mm).

For *E. coli*, a Gram-negative bacterium, the derivatives demonstrated more pronounced effects, with **AG19** exhibiting the strongest inhibition at 10 mm, followed by **AG17** (9 mm), **AG15** and **AG16** (8 mm each), **AG13** and **AG20** (8 mm each), and **AG14** (0 mm). Compounds **AG11**, **AG12**, and **AG14** were inactive against this strain. *P. aeruginosa*, another Gram-negative pathogen known for its intrinsic resistance, was inhibited by a subset of compounds, with **AG18** showing exceptional activity at 17 mm, **AG19** at 11 mm, **AG17** at 8 mm, **AG20** at 9 mm, and **AG15** at 7 mm. **AG11-AG14** and **AG16** were ineffective against *P. aeruginosa*.

As a benchmark, Streptomycin produced consistent zones of 7 mm across all strains, underscoring its reliable broad-spectrum activity. The observed zones for the AG derivatives ranged from 0 mm to 17 mm, indicating variable efficacy that correlates with structural modifications, such as the presence of electron-withdrawing groups (e.g., nitro or halogen substituents) as discussed in the synthesis section.

Table 2: Antibacterial activities of the product (**AG11-AG20**)

Compound	***S. aureus***	***B. subtilis***	***E. coli***	***P. aeruginosa***
AG11	0	7	0	0
AG12	0	0	0	0
AG13	0	6	8	0
AG14	0	7	0	0
AG15	0	0	9	7
AG16	0	7	8	0
AG17	0	6	9	8
AG18	0	0	0	17
AG19	0	8	10	11
AG20	0	9	8	9
Streptomycin	7	7	7	7

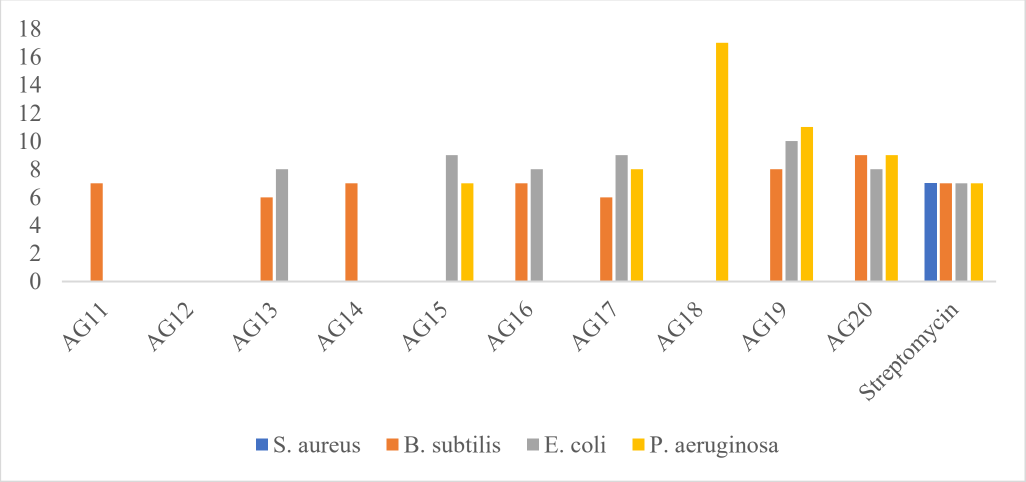

Figure 1: Antibacterial activities of the product (**AG11-20**)

The antifungal activities of the synthesized compounds **AG11–AG20** were evaluated against two yeast strains, *Candida albicans* and *Saccharomyces cerevisiae*, with fluconazole employed as a standard reference. The results, summarized in **Table 3**, reveal that most derivatives exhibited varying degrees of inhibitory effects, with several compounds demonstrating enhanced antifungal potential relative to fluconazole.

Against *Candida albicans*, compounds **AG15** and **AG16** showed the most pronounced antifungal activity, producing inhibition zones of 13 mm and 17 mm, respectively, clearly surpassing fluconazole, which exhibited a 7 mm zone. Other derivatives such as **AG14** and **AG18** also demonstrated moderate activity with zones of 9 mm and 8 mm, respectively. Some compounds, including **AG11**, **AG12**, and **AG20**, did not show measurable activity, indicating structural influences on bioactivity. These results suggest that specific substituents in the acetophenone derivatives significantly contribute to the interaction with fungal targets, enhancing antifungal efficacy.

Regarding *Saccharomyces cerevisiae*, the antibacterial profile was similarly variable. **AG14** and **AG18** showed the greatest activity, each yielding 11 mm zones of inhibition, outperforming fluconazole's 8 mm. **AG13**, **AG19**, and **AG11** also exhibited appreciable antifungal effects with zones ranging from 9 to 10 mm. Conversely, **AG12** and **AG20** showed the least activity with zones of 7 mm, comparable to or slightly below the fluconazole reference. The differential activity across the derivatives suggests that electron-withdrawing or donating substituents, steric factors, and molecular planarity influence compound-fungal cell interactions or membrane permeability, consistent with established structure-activity relationships in antifungal research.

The superior activity of **AG16** against *C. albicans* is noteworthy, indicating that its specific substitution pattern may facilitate increased cell uptake or stronger binding affinity to essential fungal enzymes or membrane components. This aligns well with literature reports where heterocyclic compounds with electrophilic centers mediate antifungal activity by inducing apoptosis-like pathways or disrupting membrane integrity. Furthermore, some derivatives outperformed fluconazole, a widely used antifungal agent, highlighting their potential as novel therapeutic candidates, especially pertinent amid growing resistance concerns.

These findings underscore the importance of molecular modifications in optimizing antifungal agents and provide a foundation for further pharmacological and mechanistic studies. Future work should include evaluating minimum inhibitory concentrations, examining cytotoxicity profiles in mammalian cells, and elucidating modes of action through biochemical assays and molecular docking. Collectively, the observed antifungal efficacy of these pyrrolo[2,3-d]pyrimidine-based hydrazone derivatives offers promising avenues for developing potent antifungal therapeutics.

Table 3: Antifungal activities of the product (**AG11-20**)

Compound	***Candida albicans***	***Saccharomyces cerevisiae***
AG11	0	9
AG12	0	7
AG13	8	10
AG14	9	11
AG15	13	9
AG16	17	8
AG17	6	8
AG18	8	11
AG19	7	10
AG20	0	7
Fluconazole	7	8

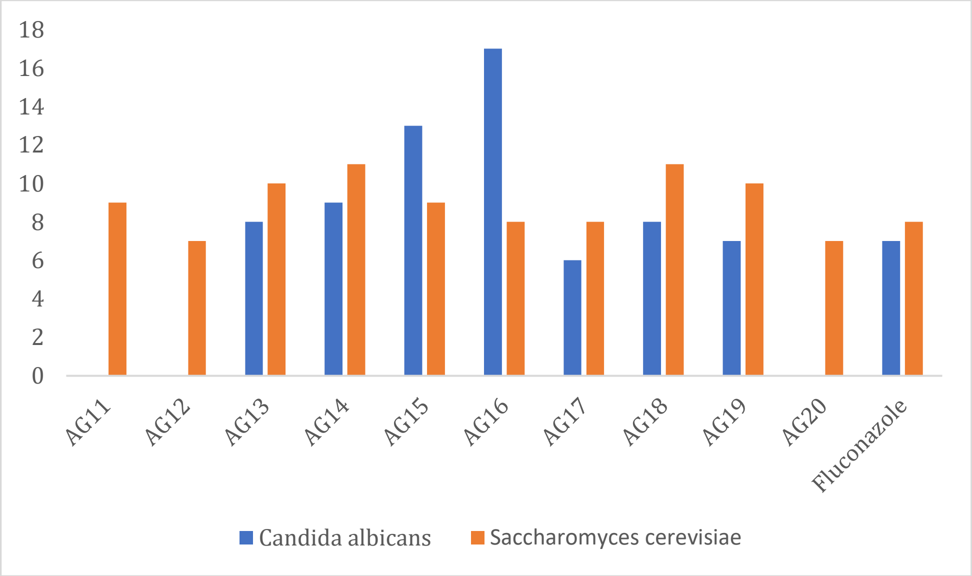

Figure 2: Antibacterial activities of the product (**AG11-20**)

Cytotoxic study:

Bioactive compounds often exhibit toxic effects on shrimp larvae, posing a potential risk to these organisms. To evaluate the in vivo lethality of such compounds on shrimp larvae (Artemia salina), the Brine-Shrimp Mortality Assay was utilized, as described in reference [24]. The results were analyzed using the LD_{50} algorithm, which facilitated the calculation of LD_{50} values along with their corresponding 95% confidence intervals, providing a robust measure of toxicity [25]. The findings, detailed in **Table 4**, highlight the eight compounds that demonstrated the most pronounced cytotoxic effects on various cancer cell lines, underscoring their potent biological activity. The shrimp lethality assay serves as a highly effective and versatile preliminary screening tool for assessing the toxicity of a wide range of substances, including heavy metals, cyanobacterial toxins, pesticides, dental material cytotoxicity, plant extract toxicity, fungal toxins, and other natural and synthetic organic compounds, enabling researchers to identify potential hazards early in the development process [24].

Table 4: Brine shrimp bioassay of **AG11-20** compounds

Compound	**LD_{50} (M)**
AG11	$>15.50 \times 10^{-4}$
AG12	$>5.50 \times 10^{-4}$
AG13	$>8.50 \times 10^{-4}$
AG14	$>20.50 \times 10^{-4}$
AG15	$>7.00 \times 10^{-4}$
AG16	$>3.75 \times 10^{-4}$
AG17	$>15.50 \times 10^{-4}$
AG18	$>3.50 \times 10^{-4}$
AG19	$>22.00 \times 10^{-4}$
AG20	$>10.75 \times 10^{-4}$

Furthermore, studies have shown a notable correlation between acute oral toxicity data in humans and rats and the outcomes of toxicity tests conducted on Artemia salina, as referenced in [26]. The results obtained from the A. salina toxicity assays were generally consistent with the toxicity data derived from rodent models, indicating a reliable alignment between these testing platforms. Notably, aquatic invertebrate assays, such as the A. salina toxicity test, demonstrated a slightly superior predictive capability for assessing acute oral toxicity of synthetic compounds in humans compared to equivalent tests conducted on rats, highlighting their utility in toxicological screening [26]. To mitigate any potential toxicity concerns arising from the solubility of compounds or the inherent toxicity of dimethyl sulfoxide (DMSO), all test substances were carefully dissolved in DMSO within the recommended volume ranges to ensure accurate and safe testing conditions. As presented in **Table 4**, the results indicate that compounds **AG12**, **AG13**, and **AG15** exhibited no harmful effects on the tested organisms, confirming their non-toxic nature under these conditions. In contrast, compounds **AG16** and **AG18** were identified as toxic, demonstrating significant poisonous effects on the organisms, thus warranting further investigation into their safety profiles.

CONCLUSIONS:

In this comprehensive study, three highly efficient, streamlined, and practical methodologies for the one-pot synthesis of dihydropyrano[2,3-c]pyrazole derivatives have been meticulously developed and elaborated upon, significantly advancing the synthetic approaches available for these valuable heterocyclic compounds. These innovative protocols are distinguished by their remarkably clean reaction profiles, which minimize the formation of byproducts and reduce environmental impact, aligning with the principles of green chemistry. The methods are designed to be user-friendly, requiring straightforward operational procedures that can be readily implemented in standard laboratory settings without the need for specialized equipment or extensive technical expertise. A key advantage of these techniques lies in their reliance on widely available and cost-effective starting materials, making them economically viable and accessible to a broad range of researchers and institutions.

These starting materials, which include common reagents such as benzaldehydes, malononitrile, phenyl hydrazine, and ethyl acetoacetate, are not only inexpensive but also commercially abundant, ensuring scalability and reproducibility of the synthetic processes. Furthermore, the protocols consistently deliver good to outstanding yields, with many reactions achieving near-quantitative conversion, thereby maximizing product output while minimizing waste. This combination of efficiency, simplicity, affordability, and high performance positions these methods as highly attractive options for the synthesis of dihydropyrano[2,3-c]pyrazole derivatives, offering significant potential for applications in medicinal chemistry, materials science, and other fields where such heterocycles are of interest.

References:

1. S.S. Murphre, “Heterocyclic dyes: Preparation, properties, and applications”, in “Progress in Heterocyclic Chemistry”, Elsevier: Amsterdam, The Netherlands, 2011, 22, p. 21-58.
2. C. Lamberth and AG20. Dinges, “The significance of heterocycles for pharmaceuticals and agrochemicals”, in “Bioactive Heterocyclic Compound Classes: Agrochemicals”, Wiley-VCH Verlag GmbH & Co. KGaA: Weinheim, Germany, 2012.
3. S. Maddila, R. Pagadala and S.B. AG20onnalagadda, Lett. Org. Chem., 2013, 10, 693-714.
4. Abdelatty, M. M., Farag, Z. R., Yossef, A. M., & Makhlouf, A. A. (2023). Synthesis, characterization, in vitro antibacterial, and molecular modeling study of some pyrazole and pyranopyrazole derivatives. *Fayoum AG20ournal of Agricultural Research and Development*, *37*(3), 478-493.
5. Shukla, P., Sharma, A., Fageria, L., & Chowdhury, R. (2019). Novel spiro/non-spiro pyranopyrazoles: eco-friendly synthesis, in-vitro anticancer activity, DNA binding, and in-silico docking studies. *Current Bioactive Compounds*, *15*(2), 257-267.
6. Reddy, G. M., Sravya, G., YuvaraAG20a, G., Camilo, A., Zyryanov, G. V., & Garcia, AG20. R. (2018). Highly functionalized pyranopyrazoles: synthesis, antimicrobial activity, simulation studies and their structure activity relationships (SARs). *Research on Chemical Intermediates*, *44*, 7491-7507.
7. Faidallah, H. M., & Rostom, S. A. (2017). Synthesis, anti-inflammatory activity, and cOX-1/2 inhibition profile of some novel non-acidic polysubstituted pyrazoles and pyrano [2, 3-c] pyrazoles. *Archiv der Pharmazie*, *350*(5), 1700025.
8. Asnani, A. (2020). In silico studies of pyrano [2, 3-c] pyrazoles derivatives as cyclooxygenase-2 inhibitiors. *GSC Biological and Pharmaceutical Sciences*, *11*(01), 166-170.
9. Faidallah, H. M., & Rostom, S. A. (2017). Synthesis, anti-inflammatory activity, and cOX-1/2 inhibition profile of some novel non-acidic polysubstituted pyrazoles and pyrano [2, 3-c] pyrazoles. *Archiv der Pharmazie*, *350*(5), 1700025.
10. Mowlazadeh Haghighi, S., Fathalipour, M., Abbasi, M., Purkhosrow, A., Oftadehgan, S., Khalafi-Nezhad, A., & Sattarinezhad, E. (2023). Synthesis, Evaluation of Vasorelaxant Activity, and Molecular Docking of Pyranopyrazole Derivatives as Calcium Channel Blockers. *Trends in Pharmaceutical Sciences*, *9*(2), 105-112.
11. Amer, M. M., Abdellattif, M. H., Mouneir, S. M., Zordok, W. A., & Shehab, W. S. (2021). Synthesis, DFT calculation, pharmacological evaluation, and catalytic application in the synthesis of diverse pyrano [2, 3-c] pyrazole derivatives. *Bioorganic Chemistry*, *114*, 105136.
12. Addoum, B., El Khalfi, B., Derdak, R., Sakoui, S., Elmakssoudi, A., & Soukri, A. (2022). Synthesis, in vitro Antimicrobial Activity, and Docking Studies of some Pyrano [2, 3-c] Pyrazole Derivatives. *Biointerface Res. Appl. Chem*, *12*, 4705-4730.
13. B.P. Bandgar, H.V. Chavan, L.K. Adsul, V.N. Thakare, S.N. Shringare, R. Shaikh and R.N. Gacche, Bioorg. Med. Chem. Lett., 2013, 23, 912-919.
14. K.M. Kasiotis, E.N. Tzanetou, and S.A. Haroutounian, Front. Chem., 2014, 2, 78.
15. M.AG20. Genin, C. Biles, B.AG20. Keiser, S.M. Poppe, S.M. Swaney, W.G. Tarpley, Y. Yagi and D.L. Romero, AG20. Med. Chem., 2000, 43, 1034-1040.
16. F. Abrigach and R. Touzani, Med. Chem (Los Angeles)., 2016, 6, 292-298.
17. A.V. Stachulski, N.G. Berry, A.C.L. Low, S.L. Moores, E. Row, D.C. Warhurst, I.S. Adagu and AG20.F. Rossignol, AG20. Med. Chem., 2006, 49, 1450-1454.
18. C.AG20. Shishoo, M.B. Devani, V.S. Bhadti, S. Ananthan and G.V. Ullas, Tetrahedron Lett., 1983, 24, 4611-4612.
19. M. Fatahpour, F. Noori Sadeh, N. Hazeri, M.T. Maghsoodlou and M. Lashkari, AG20. Iran. Chem. Soc., 2017, 14, 1945-1956.
20. M. Fatahpour, F. Noori Sadeh, N. Hazeri, M.T. Maghsoodlou, M.S. Hadavi and S. Mahnaei, AG20. Saudi Chem. Soc., 2017, 21, 998-1006.
21. M. Fatahpour, N. Hazeri, M.T. Maghsoodlou and M. Lashkari, Polycycl. Aromat. Comp., 2017, DOI: 10.1080/10406638.2017.1326948.
22. P. Dastoorani, M. T. Maghsoodlou, M. A. Khalilzadeh, and E. Sarina, Tetrahedron Lett., 2016, 57, 314-316.
23. S.S. SaAG20adikhah, M.T. Maghsoodlou and N. Hazeri, Chin. Chem. Lett., 2014, 25, 58-60.
24. A. U. Rahman, M. I. Choudhary, W. AG20. Thomsen, Bioassay Techniques for Drug Development, Harwood Academic, Amsterdam, The Netherlands, 2001.
25. B. Brayn, M. Timothy, S. Tore, General and Applied Toxicology, 2nd ed., vol. I, 52 p.
26. M. CalleAG20a, G. Persoone, Atla. 1992, 20, 396–405.